

# **HIGH SPEED UWB IN-CAR WIRELESS CHANNEL MEASUREMENTS**

**I.J. Garcia Zuazola<sup>1,2,\*</sup>, J.M.H. Elmirghani<sup>1</sup>, and J.C. Batchelor<sup>2</sup>**

This paper is a postprint of a paper submitted to and accepted for publication in *IET Communications* and is subject to Institution of Engineering and Technology Copyright. The copy of record is available at IET Digital Library

<sup>1</sup>*Institute of Advanced Telecommunications,  
University of Wales Swansea,  
Swansea, Wales, SA2 8PP, UK*

<sup>2</sup>*Department of Electronics,  
University of Kent,  
Canterbury, Kent, CT2 7NT, UK*

*\*Email: igarcia@theiet.org*

## **Abstract:**

Among the different wireless solutions *Ultra wide band* UWB is a promising technology for in-car communications due to its high data rates. To optimise the UWB radio system design, knowledge of the propagation channel within the car is required. A study of the performance of a high speed 480Mbps UWB radio system is reported here within a real in-car environment measured under mobility.

A comprehensive set of measurements is presented including several possible *Non-Line Of Sight* (NLOS) scenarios while the vehicle is stationary and mobile, for open and closed window environments and with/without occupants. These measurements are used to characterise the in-car channel and evaluate the performance of a typical UWB radio system in this setting.

## **1 Introduction**

*Ultra WideBand* (UWB) technology has gained huge interest globally due to its potential to deliver high data rate and spatial capacity, with multipath immunity [1, 2] and low power, low cost design. The deployment of this wireless technology in vehicles will provide mobility and connectivity to a host of passenger devices while reducing significantly the costs associated with wiring.

The two most common implementations of UWB systems are based on *impulse* or *MultiBand* techniques. Impulse-based UWB radio uses narrow pulses to transmit the

information, and a typical example for this approach is Direct Sequence UWB (DS-UWB). The multiband implementations of UWB (MB-UWB) split the spectrum into sub-bands and use conventional narrow band techniques, such as OFDM, to transmit the information in each sub-band [3].

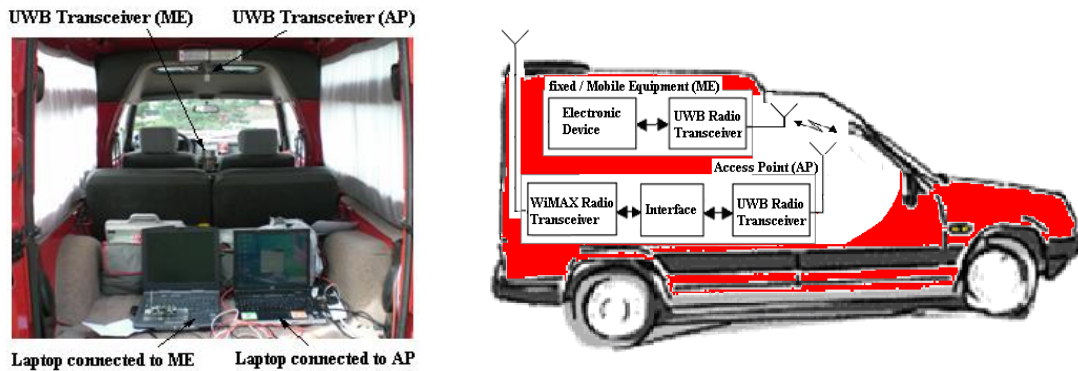


Figure 1 - The experimental set up in a typical in-car wireless channel

There are two different, competing, specifications for UWB systems in the IEEE 802.15 proposals. The proposals for a common standard were, however, withdrawn by the IEEE 802.15 Working Group. Both the DS-UWB and the MB-OFDM systems present similar characteristics for Bit Error Rate (BER); but the last system is slightly more immune to Gaussian noise [4]. Most large manufacturers of UWB chips such as Wisair and Alereon among others favour MB-OFDM (with three 528MHz sub-bands) which promises existing higher data rates than the DS-UWB based systems.

Although a fast growing competitor, the IEEE802.11n standard does not promise the same high data rates as IEEE802.15.3a [2, 5] and this is the main reason UWB is studied within the in-car environment in this work.

In this paper, radio propagation is studied using the two reciprocal techniques, time domain and frequency domain [6, 7] utilising whichever is more convenient during

the practical experiments. Channel measurements in real mobile environments are needed to overcome the lack of propagation models for this application and it is intended that the knowledge gained from this study may be used to characterise such channels.

## 2 Experimental set-up

For the in-car system set-up, a DV9110 Development Kit (DVK) from Wisair Ltd based on MB-OFDM technology was used.

A Renault Extra Van is used as a base for the experiments, Fig.1. The Wisair kit is composed of two UWB transceivers located in the vehicle. One was used as an Access Point (AP) and the other as fixed/Mobile Equipment (ME). Both transceivers used monopole antennas with 2 dBi gains. The transceiver emits a short pulse of output power  $80\mu\text{W}$  (Power Spectral Density PSD of  $-42\text{ dBm/MHz}$  max) containing the WiMedia/MBOA Group 1 sub-band (3.168 – 4.752 GHz) and using a modulated signal MB-OFDM (QPSK) at a varying physical data rate between 53.3 Mbps and 480 Mbps. Each transceiver is connected to a laptop for control and datalogging. The experimental set up and high-level block diagram for the in-car system is depicted in Fig.1.

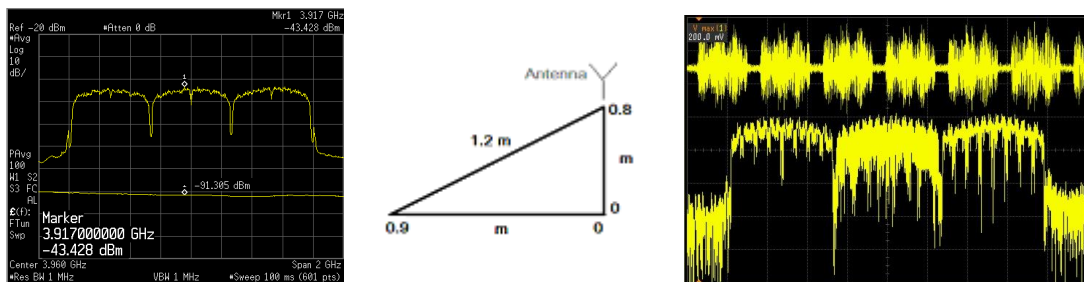


**Figure 2 – a) Spectrum Analyzer PSD b) AP location c) Oscilloscope waveform**

The wireless propagation channel studied for the specified car is of 0.9 metre radius. This is due to the AP being set in the middle of the ceiling of the car. This is the preferred location in vehicles [8] to ensure high bit rates by ensuring a good power distribution to likely Mobile Equipment (ME) locations within the car while minimizing field exposure to occupants.

In isolation, the antennas have omni-directional patterns and radiate uniformly in the plane perpendicular to the antenna. The AP antenna is located as depicted in Fig. 2b, where the horizontal distance between the antenna and the front panel is 0.9m and the height of the antenna (car ceiling) above the equipment is 0.8m. The measurements are therefore taken at 0.8m below the ceiling which is assumed to be the most likely location for the mobile/fixed equipment.

The occupants of the in-car environment were kept static, and both an open environment (windows open) scenario and vehicle mobility were examined. Although the in-car radio equipment was kept off; the influence of external RF radio interference has not been controlled.

The following focuses on collecting and analysing various characteristics for UWB peer-to-peer links within a vehicle which included the channel temporal characteristics: delay spread and amplitudes of multipath signals; path loss; spatial/spectral capacities; and Bit Error Rate (BER) for several possible *Non-Line Of Sight* (NLOS) scenarios. Although the channel measurements include the occupants who will block the energy, independently derived models for humans using UWB are given in [9] where large-scale path loss is given by the distance measured around the

perimeter of the body, and longer impulse responses and negligible energy inside the body are observed. This gives confidence that the presence of occupants can be accounted for.

### **3 Measurements and results**

Experimental results for the previously detailed MB-UWB development system within a realistic in-car environment are presented in this section.

#### *3.1 Antenna location and Channel path loss*

Figure 3a shows insertion loss (IL) of the link and return loss (RL) of the antennas for the range of lowband UWB frequencies, and a range of scenarios (stationary, open and closed environment and zero/multiple human occupants) collected by employing an Agilent 8703B vector network analyser (VNA). The reference point for the insertion loss results is taken by bringing the two antennas in close proximity. The resulting wireless channel transfer functions in the frequency domain representing the path loss are determined by the IL (S21) whereas the mismatch or de-tuning of the AP antenna by proximity to several metallic and dielectric surfaces will be given by the RL (S11).

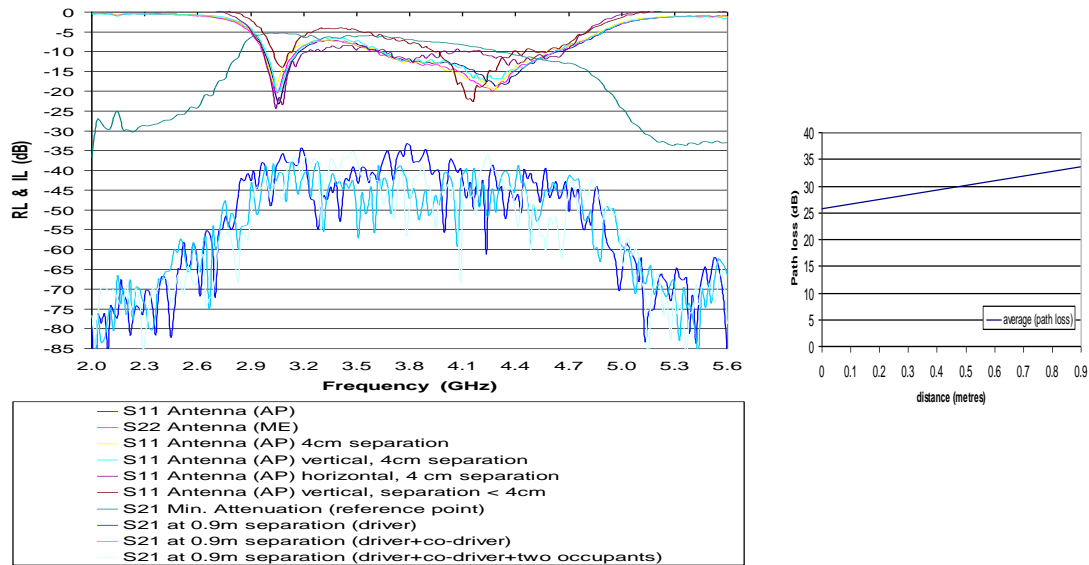


**Figure 3 - a) Antenna matching (RL) and channel path loss (IL) b) path loss**

The maximum channel path loss (where the antennas are considered as part of the channel) is measured at 33.53dB at 3.8GHz and the mismatch or de-tuning is best at about 4cm away from the metallic in-car ceiling. Figure 3b shows the average path loss over the distance of interest detailed in Fig. 2b. The results show a change in received power of 7.7dB over the measurement distance (0.9m); a significant result with respect to the short distances in-car for and given the low power spectral density (PSD) associated with UWB.

### 3.2 Signal strength and Propagation loss

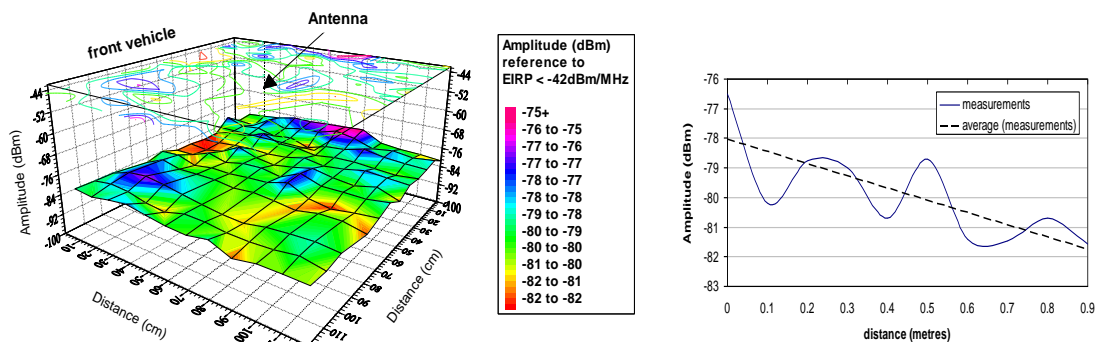


**Figure 4 – a) Signal strength vs. distance.****b) Propagation Loss**

In Fig. 4, the power measured by an Agilent E4440A PSA Series Spectrum Analyzer with good accuracy is shown when the ME antenna is moved over a grid with a 10cm spacing covering the in-car location of interest. A -91.30dBm noise floor was observed and a measured AP power of -43.42dBm (at 1MHz resolution bandwidth, RB) is employed in the UWB kit utilised as depicted in Fig. 2a.

Although the maximum power strength where the two antennas are at their closest is measured at -49.89dBm, the maximum power at the closest ME locations is -76.50dBm, and it falls to -81.55dBm for the furthest distance of 0.9m as depicted in Fig. 2b.

The channel path loss is calculated from Equation 1:

$$L_S = (P_R + G_R) - (P_T + G_T) \quad \text{Eq.1.}$$

where  $(P_R + G_R)$  is the Effective Isotropic Radiated Power (EIRP) received and  $(P_T + G_T)$  is the EIRP transmitted.

This gives a channel path loss of 38.13dB over the maximum range of 0.9m with a variation in loss of 5.05dB between the closest ME location and the maximum range.

The calculation from the measurements in Fig. 4 show agreement with the Fig. 3 results where the measured channel path loss is 33.53dB and loss variation over the closest ME location and maximum range is 7.7dB.

The DVK incorporates a Detect And Avoid (DAA) mechanism to protect Broadband Fixed Wireless Access (BFWA) systems. Although power spectral densities greater than -85dBm/MHz are available, a very low PSD of -42 dBm/MHz is used to avoid interference to systems, such as C-band satellite Digital Television (DTV) which utilise the 3.7GHz – 4.2 GHz band among others.

### 3.3 *UWB impulse response*

Figure 5 shows the effect of channel impairments on a selected part of the UWB modulated radio pulse waveform at the receive antenna. The original transmitted pulse is also shown for comparison.

An Agilent 54855A DSO Infinium oscilloscope is used for this UWB pulse sounding method to measure the channel impulse response in the time domain. The oscilloscope scale is set to 10mV and 1ns and measurements are taken at the furthest distance allowed (0.9m) between antennas for several scenarios which are described in the graph legend in Fig. 5. An example waveform of 6 groups of information is shown in Fig. 2c.

A low noise amplifier has been used at the receiver to compensate the losses associated with the channel given the very low PSD of UWB which is below the conventional receiver noise floor. A trigger mode was set to correlate the received waveforms.

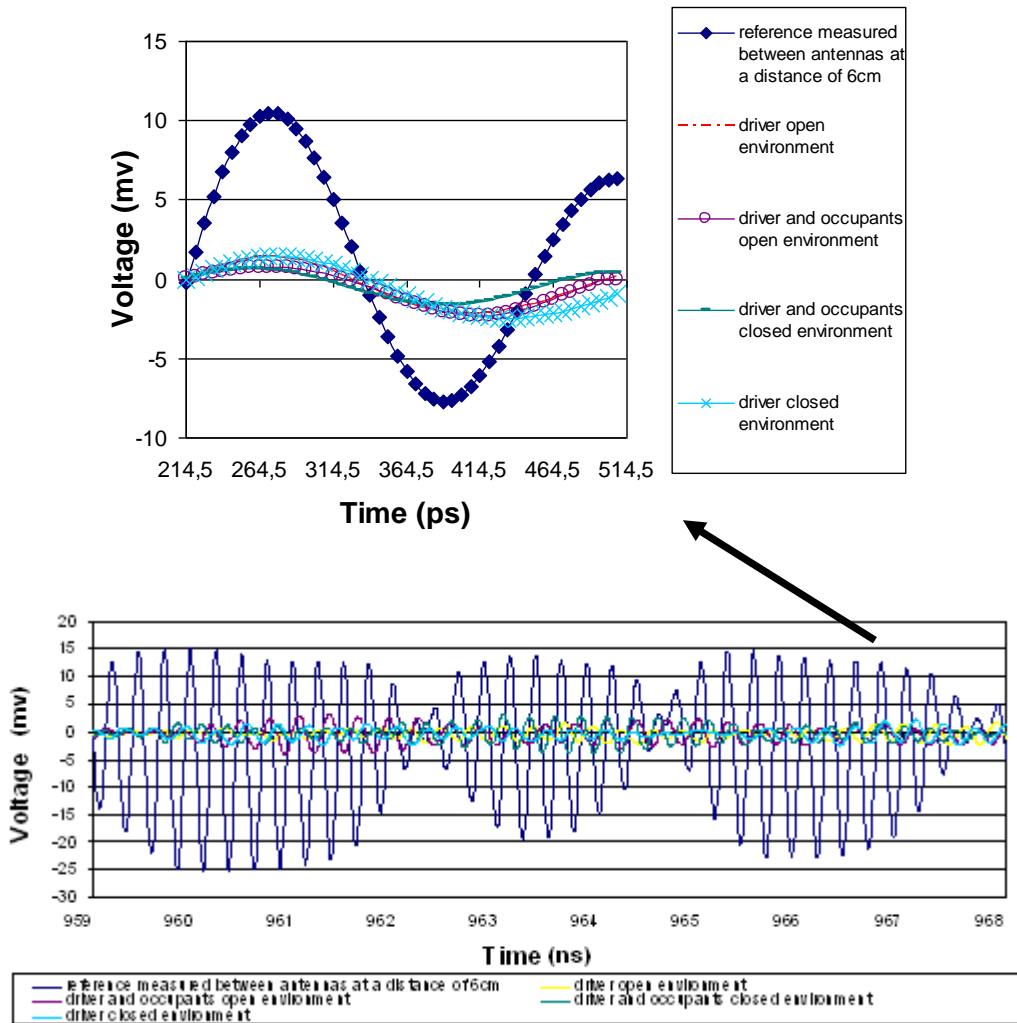


**Figure: 5** Transmitted and received UWB pulse over an in-car wireless channel, (top) over a time 214-515ps and (bottom) in wider observation over 959-968ns.

Figure 6, shows the evolution of the UWB impulse response over the in-car propagation channel using the closed environment scenario (windows closed).

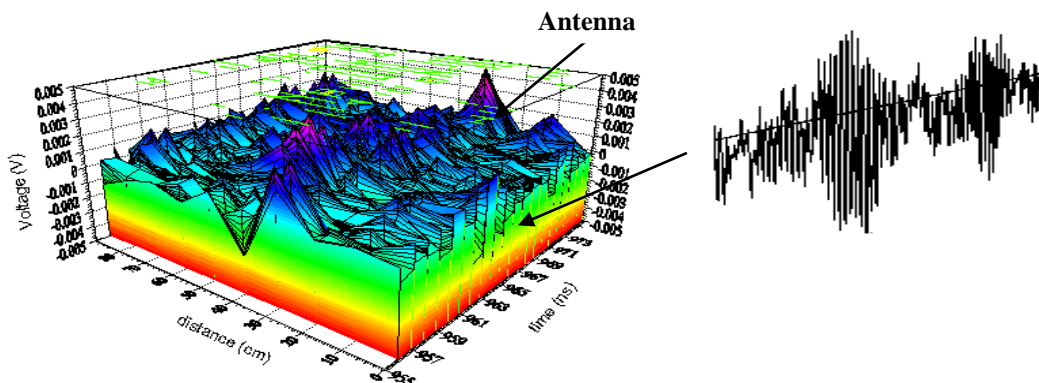


**Figure: 6 Evolution of the UWB impulse response over the in-car wireless channel. 100mV and 1ns scales are used.**

As expected and seen in Figs. 5 and 6, the signal decays with distance where an overall decrease of 13.37mV is seen between the fixed reference point AP (Fig. 2b) and the furthest range of 0.9m.

It is also observed that pulses are exposed to reflections, attenuation and diffractions resulting in longer delay spreads not greater than 0.05ns and smaller amplitudes of about 9mV for a range of 0.9m in a driver closed environment.

Multipath energy capture (collection of time-dispersed signal energy) for example in a typical single-carrier multi-band architecture is usually achieved by Rake receivers with multiple arms called fingers that are quantity limited (many arms are expensive). An advantage of knowing the channel delays is that the number of Rake fingers can be limited to an optimum value. However, this is not the case in multicarrier systems in which full Fast Fourier Transformation (FTT) computation is used rather than multipath Rake reception.

### *3.4 Multipath characteristics*

The channel multipath propagation characteristics are evaluated by examining typical path delays and power delay profiles.

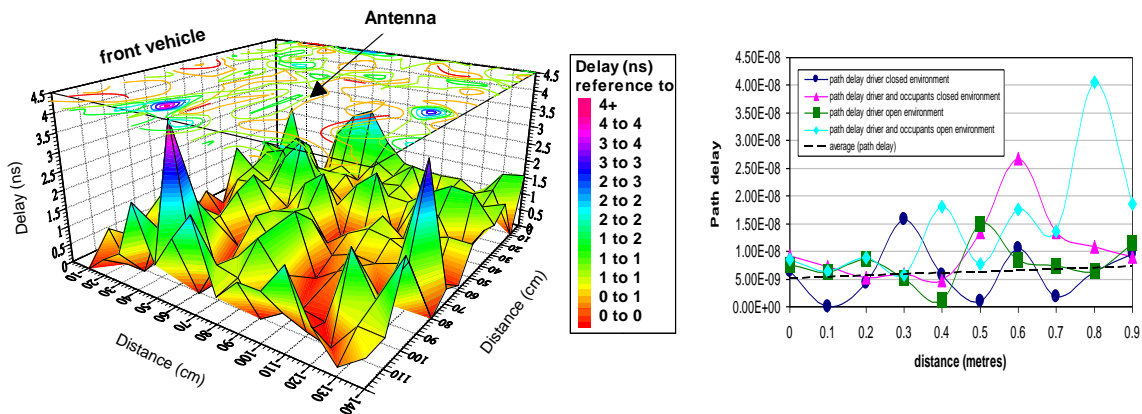


**Figure 7 – a) Path delay vs. distance.**

**b) Path delay in environment.**

Swept frequency measurement results of the channel delay were taken versus distance using a VNA. Several complex responses of the channel over a range of frequencies were measured. Readings at a 3.96GHz reference frequency are obtained and are shown in Fig. 7a. In Fig. 7b a more detailed representation of the measured delay for certain scenarios is given, showing a particularly high delay caused by the driver and occupants in an open environment compared to a driver in a closed environment scenario.

The graph in Fig. 7a shows an average delay of 2ns and in Fig. 7b the maximum path delay seen (at 0.9m) between the two extreme conditions (the driver and closed environment scenario compared to the driver and occupants in an open environment) is 8ns.

This indicates a potential increase in BER for the open environment scenarios.

UWB benefits from relative immunity to multipath fading and is capable of resolving multipath components with differential delays of 133ps [10] which implies that the existing multipath within this application can be resolved.

### 3.5 Power delay profile

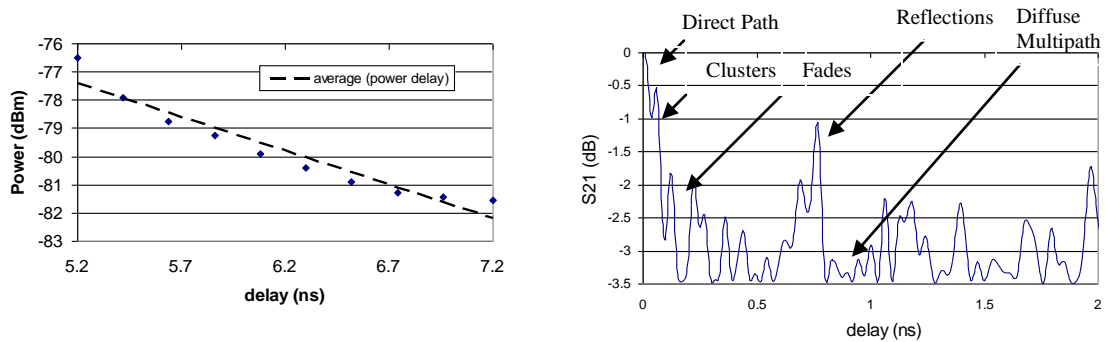


**Figure 8 – a) Power delay profile**

**b) PDP Impulse response**

In Fig. 8a the power delay profile is plotted by averaging the power readings previously observed at different delays. Excess delay is limited to 7.2ns in the desired distance of 0.9m. Figure 8b depicts the power delay profile (PDP) of the channel impulse response measured by the VNA frequency response mode at the desired distance of 0.9m and in the driver closed environment scenario. The results were obtained through an inverse Fourier transformation. According to [8] the channel characterization and the statistical radio channel models can be obtained from the impulse response. It is observed in Fig. 8b that propagation is largely immune to multipath-fading due to the broadband nature of the signal.

Although multipath in this application can be considered a useful effect allowing more signal power to be collected; high reflections (caused mainly by the small car

metallic chamber) result in Inter-Symbol Interference (ISI), which is a drawback that needs to be considered. Therefore the BER at different data rates was measured.

### *3.6 Physical Rate*

Initially, the DVK was set to a PHY Rate of 400Mbps after initial experiments demonstrated that the maximum data rate of 480Mbps is not supported over the whole desired 0.9m radius. Figure 9a depicts the measured PHY rate achievable. The vehicle measurements were carried out in a motorway environment on a mostly cloudy day with a humidity of 82%, with westerly winds of 21km/h, according to weather news. An average data rate of 400Mbps was achieved in a closed environment scenario at speeds of 140km/h whereas this data rate was only achievable up to 50km/h for the open environment scenario as in Fig. 9b. This agrees with the experimental results in section 3.4 where a potential for higher BERs for the open environment scenarios were identified due to the path delay changes in open and closed environments. Therefore it should be reasonable to assume that some rays leave the open window apertures and are reflected back with Doppler dispersion.

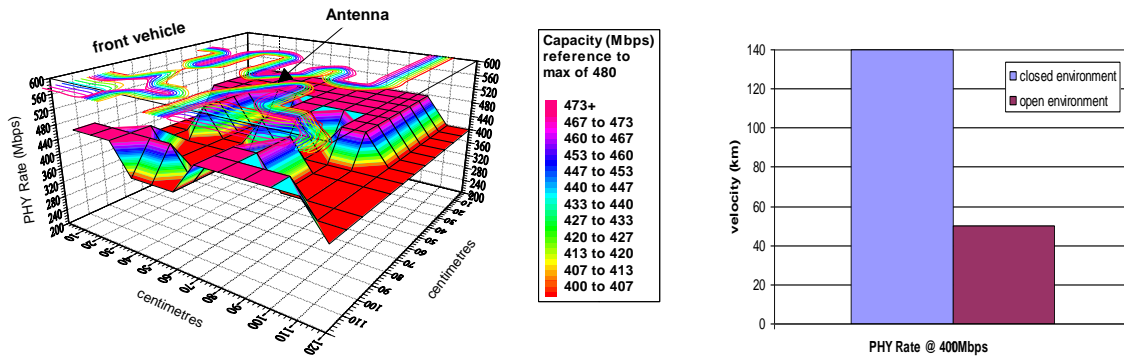


**Figure 9 –The PHY Rate achievable a) in a closed environment and b) according to velocity.**

### 3.7 Bit error rate and Capacity

The BER was then measured in a set up where the AP and ME intercommunicate reciprocally with each other. To predict the maximum achievable data rate at the allowed BER packets of certain known length are sent over the in-car channel from the AP to the ME when the vehicle was stationary and then at different vehicle velocities using the driver closed environment scenario. The received data is analyzed and recorded as BER in figures 10a and 10b respectively. Throughputs for the same set up are shown in Figs. 11a and 11b.

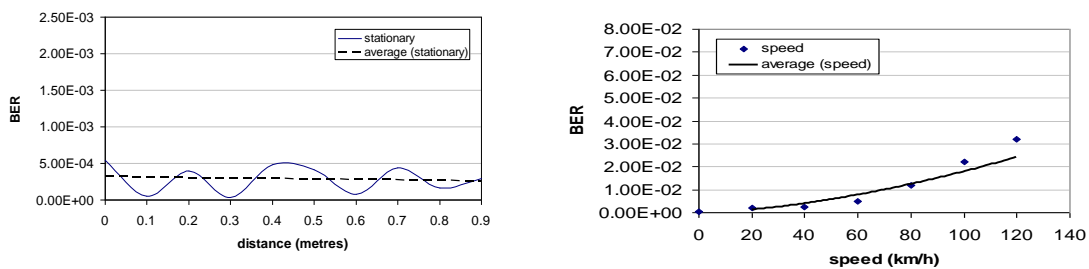


**Figure: 10 – a) The BER.**

**b) The BER vs. mobility.**

Though there are fluctuations in the BER performance, an average of  $2.5 \times 10^{-4}$  is obtained while the vehicle is stationary and BERs up to  $3.2 \times 10^{-2}$  are measured at a speed of 120km.

The intersymbol interference mainly arising from high reflections within the small car metallic chamber is conjectured to be aggravated by the antenna instability due to the mobile vehicle vibration and resulting in higher BERs as depicted in Fig. 10b.

An average of 115Mbps throughput is measured when stationary and up to 102Mbps at a speed of 120km/h.

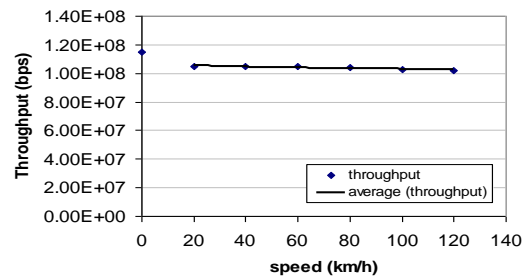
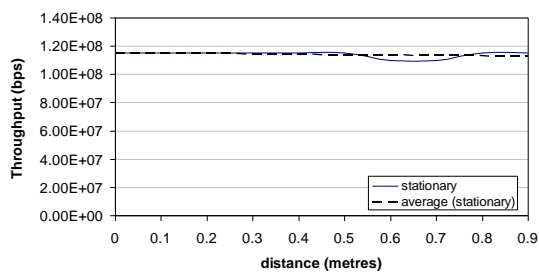


**Figure: 11 – a) Capacity vs. distance.**

**b) Capacity vs. mobility.**

#### 4 Conclusions and future work

This paper has focused on the measurements of currently unknown models describing the radio channel for a new UWB application, concluding that UWB is a very suitable and promising technology for transmission networks able to provide high data rates of 400Mbps within cars.

The results of the UWB radio channel measurements show that the radio signal attenuates a total of about 38.12dB, with 0.56dB/cm loss over the desired link distance.

It is observed that the path loss is not as expected for LOS propagation over the range within the car chamber and the main attenuation might perhaps be given by the shadowing effect. Indeed, NLOS scenarios are more common within the car than LOS propagation due to obstacles encountered mainly from the car chamber such as windows, seat bracelets (i.e the internal metallic structure of the seats [8]), and passengers.

Measurements show that an in-car UWB wireless link is more viable for a closed environment scenario, especially if high data rates are the main goal as a PHY Rate of 400Mbps is feasible. As many new cars include air conditioning, it is not unreasonable to expect the environment to be closed for the majority of the time.

The actual data rate of the UWB DVK is significantly below the PHY Rate (285Mbps in this setting). This is due to the fact that the PHY rate is sometimes also referred to as channel rate. That is, the manufacturer's advertised data rate is the maximum bit rate through the physical layer medium, not the payload bits necessary for data transmission.

LOS transmission obviously improves the system data rate meaning that potentially directional antennas such as patch arrays, Planar Inverted-F Antennas (PIFAs) [11], beam steered arrays, Electromagnetic Band Gap (EBG) antennas [11], SIMO diversity, and MIMO systems [12] could improve the overall system performance.

Equations for calculation of path loss, received signal power, channel capacity, for common UWB channel models in certain applications can be obtained from [12, 13].

## 5 Acknowledgment

This work has been part-funded by the European Union through the Welsh Assembly Government.

Many thanks to David Garcia Cayuela and Handan Inal for their support and patience during measurements and to Yossi Kolkovich (Wisair) for the technical support.

## 6 References

- [1] A. F. Molisch, et al., 'Channel models for ultrawideband personal area networks', IEEE Wireless Commun., pp. 14-20, Dec. 2003.
- [2] Suiyan Geng; Ranvier, S.; Xiongwen Zhao; Kivinen, J.; Vainikainen, P.; 'Multipath propagation characterization of ultra-wide band indoor radio channels', IEEE International Conference on Ultra-Wideband, 5-8 Sept. 2005 Page(s):11 - 15
- [3] J.M.H. Elmirghani, B. Badic, Y. Li, R. Liu, R. Mehmood, C. Wang, W. Xing, I.J. Garcia Zuazola and S. Jones, 'IRIS: AN INTELIGENT RADIO-FIBER TELEMETICS SYSTEM', 13th ITS World Congress and Exhibition in London, 8-12 October 2006.
- [4] Stephen H. Kratzet, 'MB-OFDM and DS-UWB Ultra-Wideband Design Using SystemView by Elanix®', Eagleware-Elanix App Note AN-24B Mar 30, 2005
- [5] Bob Wheeler and Joseph Byrne, 'A Guide to Next-Generation Wireless UWB, Wireless USB, 802.11n/MIMO, and WiMAX', First Edition, August 2005
- [6] Hovinen, V.; Hamalainen, M.; Patsi, T. 'Ultra wideband indoor radio channel models: preliminary results', IEEE Conference on Ultra Wideband Systems and Technologies, 21-23 May 2002 Page(s):75
- [7] U. G. Schuster and H. Bölcskei, 'Ultrawideband channel modeling on the basis of information-theoretic criteria', IEEE Transactions on Wireless Communications, 2006
- [8] T. Kayser, J. v. Hagen, and W. Wiesbeck, 'Optimisation of Antenna Locations for Wireless In-car Communication', URSI International Symposium on Electromagnetic Theory, Pisa, Italy, May 2004
- [9] Andrew Fort, Julien Ryckaert, Claude Desset, Philippe De Doncker, Piet Wambacq, and Leo Van Biesen, 'Ultra-Wideband Channel Model for Communication Around the Human Body', IEEE Journal on selected areas in communications, Vol. 24, No. 4, April 2006
- [10] A. F. Molisch, J. R. Foerster, and M. Pendergrass, 'Channel models for ultrawideband personal area networks', IEEE Personal Comm. Magazine, 2003.
- [11] Y. Hao, A. Alomainy, I. J Garcia Zuazola and C. G. Parini, 'Small Antennas on Electromagnetic BandGap Structures', PIERS 2004, Progress in Electromagnetics Research Symposium, 28-31 March 2004, Pisa, Italy
- [12] Biagi, M.; Baccarelli, E.; 'A simple multiple-antenna ultra wide band transceiver scheme for 4th generation WLAN'. IEEE 58th Vehicular Technology Conference, 2003.
- [13] Richardson, P.C.; Weidong Xiang; Stark, W.; 'Modeling of ultra-wideband channels within Vehicles', IEEE Journal on Selected Areas in Communications, Volume 24, Issue 4, Part 1, April 2006, Page(s):906